Thermal Decomposition of Some Sol-Gel Precursors for Mesoporous TiO_2-Based Thin Films for Chemorezistive Environmental Sensors

VIOLETA DEDIU[1]*, VIORICA MUSAT[2], BOGDAN JURCA[3], NICOLAE IONUT CRISTEA[1]

[1] National Research and Development Institute for Industrial Ecology ECOIND, 71-73 Drumul Podu Dambovitei Str., 060652, Bucharest, Romania

[2]Dunarea de Jos University of Galati, Centre of Nanostructures and Functional Materials-CNMF, 111 Domneasca Str., 8000201 Galati, Romania

[3] University of Bucharest, Department of Physical Chemistry, 4-12 Elisabeta Blvd., 030018, Bucharest, Romania

This paper presents a comparative study on the thermal decomposition in air and FTIR analyses of complex sol-gel precursors used for the deposition of three titania based mesoporous thin films: TiO_2, Nb-doped TiO_2 and carbon nanotubes (MWCNT)-doped TiO_2. The effect of doping with Nb or adding MWCNT on the thermal decomposition of titanium isopropoxide-based precursor and crystallization of TiO_2 was investigated through thermogravimetric analysis (TGA), differential thermal analysis (DTA), and Fourier Transform Infrared (FTIR) data. TG-DTA results showed two main exothermic peaks were observed in all samples for the temperature range 280-300 °C and 429-444 °C, corresponding to isopropoxide oxidative decomposition and anatase crystallization. In case of Nb doped TiO_2 an oxidative decomposition of Nb ethoxide appears at 198 °C. The acidified MWCNT are thermally stable up to 500°C. Doping TiO_2 causes peaks shift to higher temperatures. Also, the effect of heating rate on thermal decomposition for precursors was studied. FTIR analyses were conducted on precursor systems thermally treated at different temperature to track the chemical transformations during the films formation.

Keywords: TiO_2, TG–DTA–FTIR, Sol-gel, Functionalized MWCNT

Nanocrystalline titanium dioxide has remarkable properties with a wide range of known and potential applications. Among the major industrial applications of this material are in the pigments, plastics, cosmetics, electronics, and catalysts production. TiO_2 thin films have been studied in applications such as solar cells [1], photodecomposition of water [2], self-cleaning [3], gas sensors [4], photocatalyst [5-6] optical filters [7], antireflection coatings [8], ceramic membrane [9], antibacterial powders [10], biomedical applications [11], etc. Many papers have been published on the preparation of nano-titania using the sol–gel method [12, 13].

Porous TiO_2-based thin films obtained by sol–gel method are found to exhibit important chemoresistive properties and proved to sense gases at moderately low temperature range (200–400 °C). In order to increase the sensitivity and/or selectivity of the sensing materials, the properties of titania can be optimized by doping with small amount of donor (Nb^{5+}, V^{5+}, Pt^{6+}) or acceptor type (Cr^{3+}, La^{3+}) ions [14-18]. Multiwalled carbon nanotubes (MWCNTs), having high electrical conductivity even at room temperature and large surface area, when added to TiO_2 matrix, can provide good and fast response to gas presence at low temperature range [19-20].

The aim of this article is a better understanding of the formation mechanism of mesoporous titania doped with Nb and MWCNT, materials used in gas sensor applications. For this propose, thermal analysis (TG-DTG-DTA) and FTIR spectroscopy have proved useful techniques. The information obtained from these analyses would enable an optimization of the Nb-TiO_2 and MWCNT-TiO_2 synthesis in order to obtain high gas sensing performance.

Experimental part

Materials

Titanium isopropoxide Ti (i-$OC_3H_7)_4$ (TIP, 97%), acetyl acetone (AcAcH, ≥99.6%), triblock copolymer Pluronic P-123 ($EO_{20}PO_{70}EO_{20}$), ethanol (>99.9%) were purchased from Aldrich and used as received. Niobium ethoxide (>99.8%) was used as niobium oxide source (Strem Chemicals). Hydrochloric acid (37%), nitric acid (100%) and sulphuric acid (98%) were purchased from Merck. Commercially available (Nanocyl, S.A.) multiwalled carbon nanotubes were used. The row nanotubes had their outer and inner diameters of about 15 nm and 7 nm, respectively.

Sample preparation

In order to achieve homogeneous dispersion of MWCNTs into TiO_2 matrix, the MWCNT powder was treated with a mixture of H_2SO_4 and HNO_3 and boiled at 120°C for 50 min. After that, the carbon nanotubes were filtered and washed with deionized water until reach a *p*H of 7.0. The resulting powder MWCNT was dried at 60°C and re-suspended in ethanol by ultrasonication.

For the non-doped sample, 2.8 g of titanium isopropoxide (Ti (i-$OC_3H_7)_4$, TIP) was added dropwise to a solution of small amounts of hydrochloric acid, water and acetyl acetone dissolved in ethanol, under vigorous magnetic stirring. The well-mixed solution was kept stirring at room temperature for 1 h to obtain the solution A. In a separated beaker, Pluronic P123 was dissolved in ethanol thoroughly under vigorous magnetic stirring to obtain the solution B. The solution B was slowly added to the solution A, and the mixed solution was continuously stirred at ambient temperature for another hour. The resultant sol was then used to cover the glass substrate through spin coating technique. All these operations were performed inside of glove box in a controlled environment (nitrogen, RH<15%). The glass slide was cleaned in ultrasonic bath with detergent, acetone and ethanol and dried with nitrogen.

The Nb (1 wt. %)-doped TiO_2 sample was synthesized through a similar sol–gel route; the difference was the addition of a solution of niobium alkoxide precursor

* *email: violeta.dediu@incdecoind.ro*

dissolved in ethanol that was added in solution A. For the MWCNT (0.1 wt. %) doped sample, a solution of MWCNT dispersed in ethanol was added to the solution A.

The samples prepared for TGA and DTA were dried at 100 °C for 1h, for FTIR analyses the powders were mixed with KBr. For some samples different initial thermal treatments were carried out in order to emphasize the changes in samples composition.

Characterization and measurements

The TG-DTA analysis was carried out in air using different heating rates, from room temperature to 1000 °C, using Rigaku equipment (model 8121 BH). For the thermal characterization, different thermogravimetry and differential thermal analysis analyses were performed. The FTIR spectra were obtained with Perkin-Elmer spectrophotometer (model 903) in the 4000–450 cm^{-1} range with pressed KBr based pellets, working in absorbance mode.

Results and discussions

Thermal analysis of un-doped TiO_2 precursor

Figure 1 shows the TG-DTG-DTA analyses recorded for TiO_2 precursor powder. The thermogram data show that organic substances from the precursor were removed by heating up to 530°C in air. Thermal evolution takes place in four consecutive steps (fig. 1a) with weight losses for which the inflection point coincides with the temperature corresponding to the endothermic and exothermic peaks in DTA analysis. The total mass loss registered is around 65%. The weight loss begins at 60°C with release of physical absorbed water under endothermic condition and has the highest speed at 80°C, fact reflected in a peak in the DTG curve observed especially at high heating speeds. Heating furthermore the traces of hydrochloric acid evaporates in air and unreacted acetyl acetone oxidative decomposes in the air. A second step starting at 184°C corresponds to the spontaneous combustion of organic matter. This process is fast as can be seen from DTG curve, accompanied with the most significant mass loss (more than half of total mass loss). The Pluronic 123 triblock copolymer decomposes at temperatures above 330 °C, as illustrated in the DTA curve by a broad peak, best evidenced at a rate of 5 K/min, creating the network of pores in the oxide material. In the last step, the TiO_2 crystallizes in anatase phase at temperatures above 400°C.

From the shapes of DTA curves at different heating rates (fig. 1b) it can be noticed that DTA peaks move to higher temperatures with increasing heating speed. It results that crystallization in the form of anatase occurs at higher temperatures with increasing heating speed.

Thermal analysis of Nb-doped TiO_2 precursors

In the case of sol doped with Nb (1 wt. %), a supplementary step appears in thermal analysis corresponding to niobium ethoxide presence in the precursor (fig. 2). This oxidative decomposition process is very fast and runs between 160 and 240 °C.

The total mass loss is estimated to be around 75 %, higher than of the undoped precursor case, due to the higher percentage of the alkoxide radicals that decompose into the volatile components. The DTA curve does not show the peak corresponding to niobium oxide crystallization, probably it is in too small amount.

Thermal analysis of MWCNT-doped TiO_2 precursors

The precursor doped with 0.1% MWCNT was subjected to the thermal analysis according to the same protocol as for the undoped precursor. In order to highlight the effect of doping with carbon nanotubes, the thermal behavior of MWCNT was first studied. In case of multiwalled carbon nanotubes, the first mass loss step was observed at low temperature 84°C, accompanied by an endothermic small peak visible in the DTA signal, due to the release of moisture adsorbed onto surface and to HNO_3 trace in MWCNT. As revealed by the DTG curve shown in Figure 3a, the initial degradation of carboxyl starts at approximately 120 °C and reaches a maximum weight loss of the acidic group at about 168°C and completes at 480 °C accompanied with H_2SO_4 trace release. The last exothermic peak appearing at 516 °C corresponds to the MWCNT combustion, which

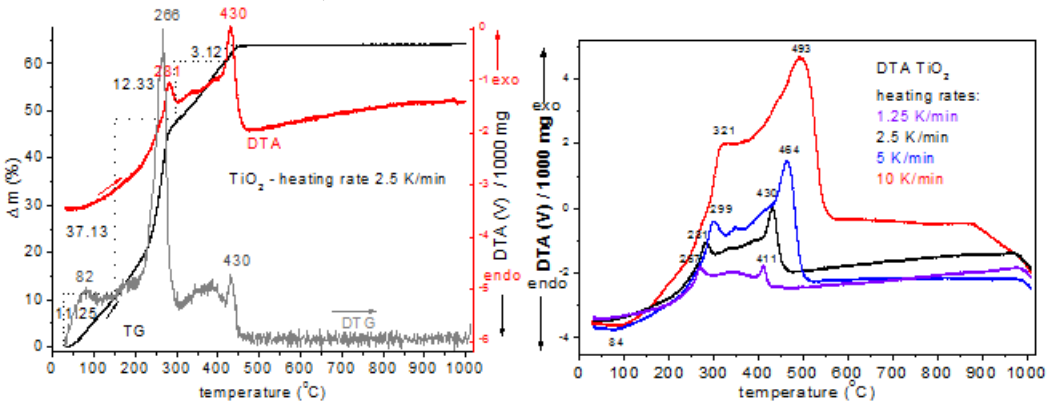

Fig. 1 (a) TG-DTG-DTA curves of dried TiO_2 precursor (b) DTA curves for TiO_2 precursor at different heating rates

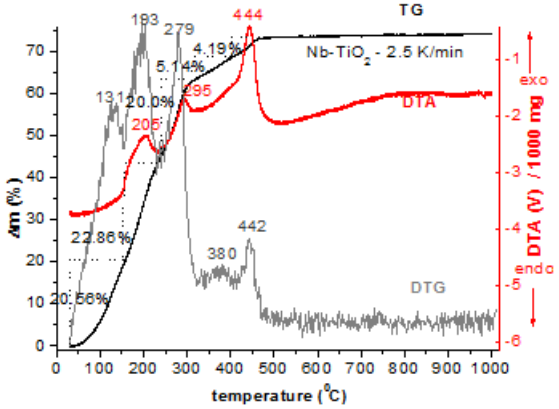

Fig. 2 TG-DTG-DTA curves of dried Nb-TiO_2 precursor

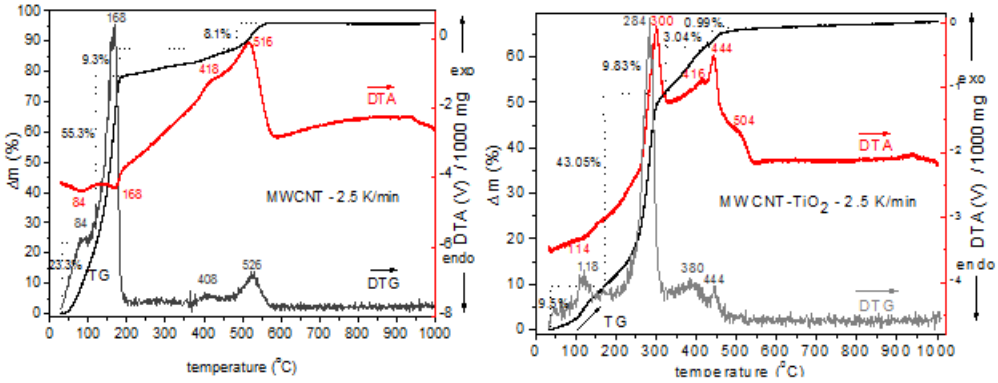

Fig. 3 Thermal behavior of (a) MWCNT °i (b) MWCNT-TiO_2 precursor

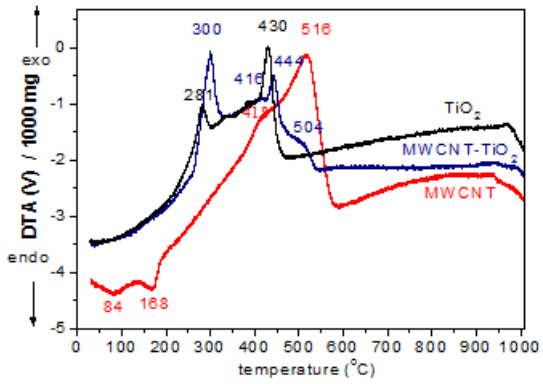

Fig.4 Comparison between thermal behaviors of MWCNT, TiO_2, MWCNT-TiO_2 precursors

is useful information in thermal treatment of composite MWCNT-TiO_2 material. The total mass loss is around 96% and the most significant loss and, at the same time the fastest stage, is between 120 and 190°C.

From figure 3 b it can be noted that there are 5 steps of mass loss for MWCNT- TiO_2 precursor, stages accompanied by thermal effects. Carboxyl groups on the surface of carbon nanotubes decompose at 416 °C, approximately the same temperature as in free nanotubes case.

The crystalline phase of the anatase begins to crystallize at higher temperatures than in the TiO_2 precursor, as illustrated by the shift to higher temperature values of the DTA peak (fig. 4). Carbon nanotubes, which are very small amount in the TiO_2 matrix, burn at 504 °C compared to the 516 °C temperature for free nanotubes, although the percentage of MWCNT in material is only 0.1%.

Effect of heating rate and doping on thermal decomposition of precursors

In all the cases the peaks for each sample shift to higher temperatures when heated at a higher rate (table 1) because all the transitions (evaporation, crystallization, decomposition, etc.) are kinetic. Also, the peaks are wider at higher heating rate. As can be seen in figure1, increasing the scanning rate increases sensitivity, while decreasing the scanning rate increases resolution. The doping of samples induces a shift of the maximum temperature to higher values.

The doping with Nb or MWCNT induces a shift of oxidative decomposition peak of the TiO_2 precursor to higher temperature and the peak associated with the crystallisation in the anatase phase also moves to higher temperatures for all heating rates.

FTIR analysis of TiO_2 samples annealed at 450 °C

Figure 5 shows the FTIR spectra of samples after heat treatment at 450 °C. The absorption spectra shows that samples contain water adsorbed with the same properties of free water molecules and a small fraction of water tightly bounded to samples, probably under hydroxyl form [21]. It can be seen the presence of a continuous absorption region of 3400-3750 cm^{-1}, an absorption band around 1618 cm^{-1} ascribed to water molecule deformation vibration and two bands at 3730 and 3660 cm^{-1} assigned to two different types of surface OH groups, which are located on different crystalline planes of TiO_2 [21-22].

The investigations in the spectral region 1300–700 cm^{-1} reveal vibrations of the surface groups [21], as a result of the hydroxyl coverage and metal–oxygen bonds on the oxide surface, and also because of the dopant. In the region 700–400 cm^{-1} a broad and intense band identified as the Ti-O bond stretching vibration (642 and 546 cm^{-1}) and Ti-O-Ti stretching vibration (498 and 420 cm^{-1}) indicates the presence of a titanium oxide network.

Table 1

DOPING AND HEATING RATE EFFECTS ON CHARACTERISTIC DTA EXOTHERMIC PEAKS POSITION FOR TiO_2 BASED PRECURSORS

Heating rate	TIP oxidative decomposition (°C)			Anatase crystallization (°C)		
(K/min.)	TiO_2	MWCNT-TiO_2	Nb-TiO_2	TiO_2	MWCNT-TiO_2	Nb-TiO_2
1.25	267	285	283	411	426	396
2.5	281	300	293	429	444	444
5	299	321	313	464	471	477
10	321	343	339	493	493	498

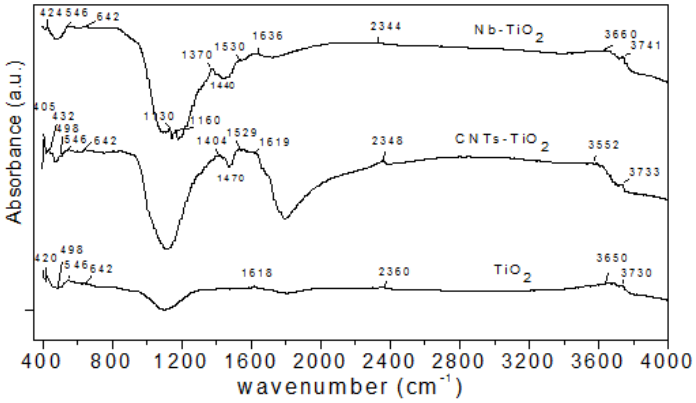

Fig.5 FTIR spectra of undoped and doped TiO_2 samples annealed at 450°C

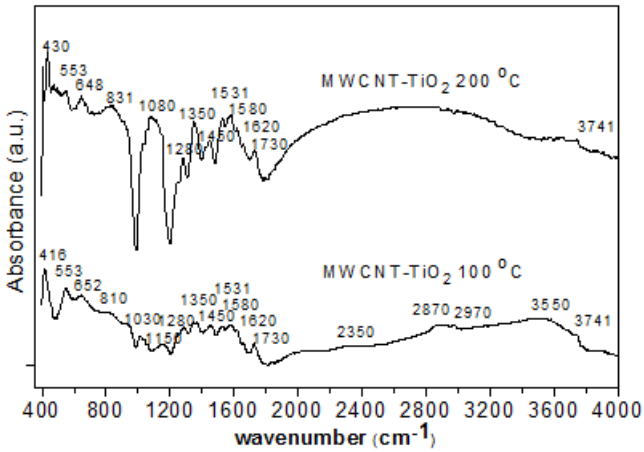

Fig.7 FTIR of MWCNT-TiO_2 samples heat treated at 100 and 200 °C

FTIR analysis of Nb-TiO_2 sample

The FTIR spectra of Nb-TiO_2 samples heat treated at 100 and 200 °C are shown in figure 6. As can be seen, the spectrum of sample treated at 200 °C is more complex. In case of Nb-doped TiO_2 the peak from 1618 cm^{-1} broaden and those at 3730 and 3650 cm^{-1} shifted with 10 cm^{-1} to higher wavenumber.

The peaks from 3500–3600 cm^{-1} domain were attributed to the presence of Pluronic 123 at temperatures below its decomposition temperature. Also it was a peak at 2853 cm^{-1} which corresponds to antisymmetric vibration modes of -CH_2- and-CH_3 groups from the alkoxide. Characteristic doublet of the gem-dimethyl structure of isopropoxides appeared at about 1375 cm^{-1}. A band consisting in two overlaped peaks at around 1528 cm^{-1} and 1565 cm^{-1} was observed. This may be assigned to the (C-C) and (C- O) stretch vibrations from the Acac rings bonded with Ti metal atoms. The characteristic bands of inorganic compounds are localized between 1000 and 400 cm^{-1}. The band at about 430 cm^{-1} can be attributed to the vibration bond (Ti-O) of the stabilized titanium isopropoxide with acetyl acetone. This indicates that acetylacetonate ligands remain bound to titanium in the sample examined by FTIR.

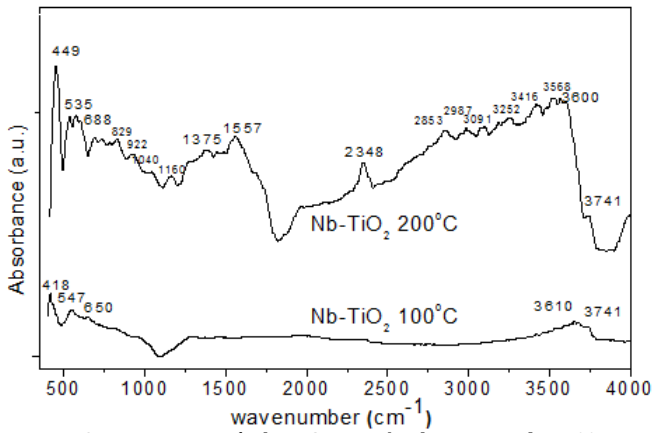

Fig. 6 FTIR spectra of Nb –TiO_2 samples heat treated at 100 and 200 °C

FTIR analysis of MWCNT-TiO_2 sample

The FTIR spectra of MWCNT-TiO_2 samples heat treated at 100 and 200 °C are shown in figure 7. Oxidation of MWCNT surface introduces carboxyl and hydroxyl groups enabling further chemical reactions. The MWCNT exhibit a strong absorbance in IR and some difficulties can appear in distinguishing them from the background noise.

In both cases it can be seen the peak for -OH groups from adsorbed water. In case of sample treated at 100° C two overlaped peaks appeared at 2970 and 2860 cm^{-1} correspond to symmetric and antisymmetric vibration modes of -CH_2- and -CH_3 groups. For the sample treated at 200° a broad band between 3400 an 1800 cm^{-1} incorporates all these peaks. Also in the FTIR spectra apears a band at 1730 asigned to C=O stretching vibration from carboxyl present on the surface of functionalized carbon nanotubes. In the spectra are presented two bans at 1580 and 1350 cm^{-1} coresponding to asymetric and symetric O-C-O stretching vibration in coordinated $HCOO^-$ from the acidified MWCNT [24]. Also, the band coresspponding to water molecules adsorbed on the surface appears at 1620 cm^{-1}. The bands around 1455 cm^{-1} are related to C-H asymmetric deformation and -CH_2- scissors vibration.

Conclusions

A comparative study on the thermal decomposition in air of complex sol-gel precursors used for the deposition of mesoporous TiO_2, Nb-TiO_2 and MWCNT-TiO_2 films was realised based on TG-DTG-DTA, and FTIR data. TG-DTA results showed that organic substances in all samples were removed and oxide passes from the amorphous phase to the crystalline phase by heating up to 500 °C in air. In all samples, two main exothermic peaks can be observed in the temperature range 280-300°C and 429-444 °C, corresponding to isopropoxide oxidative decomposition and anatase crystallization respectively. In case of Nb doped TiO_2 a supplementary step appears at 198°C because of oxidative decomposition of niobium ethoxide. Studying the acidified MWCNT thermal behavior, it can be seen that they are thermally stable bellow 500°C. Nb-doping and MWCNT-doping cause a shift to higher temperatures of the mean peaks in DTA curves and this effect was most important in the case of using niobium ethoxide as precursor for doping. Nb-doping results in a new exothermic peak at 210 °C in DTA curve.

FTIR analysis of samples thermally treated at 450°C shows the formation of crystallized oxides which is confirmed by the presence of vibration bands characteristic of Ti-O-Ti bonds in the 700-400 cm^{-1} spectral region. Hydroxyl groups, located on different crystallographic faces, especially in the case of oxides doped have been evidenced by the bands in the region 3400-3750 cm^{-1} and also physically adsorbed water (line 1618 cm^{-1}). In FTIR spectra of the samples treated at 100 and 200°C were highlighted the dimethyl-geminal structure of isopropoxide and the rings formed be acetyl acetonate and metal ions, also the characteristic lines for the Ti-O and Ti-O-Ti groups start to appear.

References

1. O'REGAN, B., GRATZEL, M., Nature, **353**, 1991, p. 737.
2. MOR G. K., SHANKAR, K., PAULOSE, M., VARGHESE, O. K., GRIMES, C. A., Nano Lett., **5**, no. 1, 2005, p. 191.
3. CHIEN, D. M., VIET, N. N., VAN N. T.i K., PHONG N. T. P., J. Exp. Nanosci., **4**, no. 3, 2009, p.221.
4. STANKOVA N.E., DIMITROV I.G., STOYANCHOV T.R., ATANASOV P.A., Appl. Surf. Sci., **254**, 2007, p. 1268.
5. NITOI I., OANCEA P., CONSTANTIN L., RAILEANU M., CRI'AN M., CRISTEA I., J. Environ. Prot. Ecol., **17**, no. 1, 2016, p. 315.
6. CONSTANTIN L.A., NITOI I., CRISTEA I., OANCEA P., Rev. Chim. (Bucharest), **67**, no. 8, 2016**,** p.1447.
7. KITUI M., MWAMBURI M. M, GAITHO F., MAGHANGA C. M., Int. J. Thin Fil. Sci. Tec., **4**, no. 1, 2015, p.17.
8. BOMMEL M.J. VAN, BERNARDS T.N.M., J. Sol-Gel Sci. Technol., **8**, 1997, p. 459.
9. AGANA A. B., REEVE D., ORBELL J. D., Desalination, **311**, 2013, p.162.
10. COPCIA V. E., HRISTODOR C. M., DUNCA S., IORDANOVA R., BACHVAROVA-NEDELCHEVA A., FORNA N. C., SANDU I., Rev. Chim. (Bucharest), **64**, no. 9, 2013, p. 978.
11. GHEORGHIEVICI G. L., TRISCA RUSU C., VOICILA E., NAFLIU I. M., CIMBRU A. M., TANCZOS S. K., Rev. Chim. (Bucharest), **68**, no. **1**, 2017, p.11.
12. RAILEANU M., CRISAN M., IANCULESCU A., CRISAN D., DRAGAN N., OSICEANU P., SOMÃCESCU S., STANICA N., TODAN L., NITOI I., Water Air Soil Pollut., **224**, 2013, p. 1773.
13. NITOI I., OANCEA P., CONSTANTIN L. A., CRISAN M., CRISAN D., CRISTEA I., CONSTANTIN M. A., International Symposium The Environment and the Industry, 2016, p.285.
14. COMINI E., FERRONI M., GUIDI V., VOMIERO A., MERLI P.G., MORANDI V., SACERDOTI M., DELLA MEA G., SBERVEGLIERI G., Sens. Actuators, B, **108**, 2005, p. 21.
15. HAN Z., WANG J., LIAO L., PAN H., SHEN S., CHEN J., Appl. Surf. Sci., **273**, 2013, p 349.
16. MARDARE D., IFTIMIE N., CRI^{a}AN M., RÃILEANU M., YILDIZ A., COMAN T., POMONI K., VOMVAS A., J. Non-Cryst. Solids, **357**, 2011, p.1774.
17. EPIFANI M., HELWIG A., ARBIOL J., DIAZ R., FRANCIOSO L., SICILIANO P., MUELLER G., MORANTE J.R., Sens. Actuators, B, **130**, 2008, p 599.
18. HIEU N.V., DUY N. V., P. T. HUY, CHIEN N. D., Physica E, **40**, 2008, p. 2950.
19. SANCHEZ M., RINCÓN M.E., Sens. Actuators, B, **140**, 2009, p. 17.
20. UEDA T., TAKAHASHI K., MITSUGI F., IKEGAMI T., Diamond Relat. Mater., **18,** 2009, p. 493.
21. YATES D. J. C., J. Phys. Chem., **65**, no. 5, 1961, p. 746.
22. LARBOT A., LAAZIZ I., MARIGNAN J., QUINSON J.F., J. Non-Crystall. Solids, **147–148,** 1992, p. 157.
23. BURGOS M., LANGLET M., Thin Solid Films, **349**, 1999, p. 19.
24. ABUILAIWI F. A., LAOUI T., AL-HARTHI M., ATIEH M. A., Arab. J. Sci. Eng., **35**, 2010, p. 37.

Manuscript received: 15.01.2017